Phase Induced Amplitude Apodization (PIAA) Coronagraphy: Recent Results and Future Prospects

Olivier Guyon*[a,b], Brian Kern[c], Ruslan Belikov[d], Stuart Shaklan[c], Andreas Kuhnert[c], Amir Giveon[c], Frantz Martinache[b]

[a] University of Arizona, Steward Observatory, 933 N. Cherry Ave., Tucson, AZ 85721, USA;
[b]Subaru Telescope, National Astronomical Observatory of Japan, 650 N. A'ohoku Place, Hilo, HI 96720, USA;
[c]Jet Propulsion Laboratory, California Institute of Technology, 4800 Oak Grove Drive, Pasadena, CA 91109, USA;
[d]NASA Ames Research Center, Moffet Field, Mountain View, CA 94035, USA

ABSTRACT

Thanks to the use of aspheric optics for lossless apodization, the Phase Induced Amplitude Apodization (PIAA) coronagraph offers full throughput, high contrast and small inner working angle. It is therefore ideally suited for space-based direct imaging of potentially habitable exoplanets. The concept has evolved since its original formulation to mitigate manufacturing challenges and improve performance. Our group is currently aiming at demonstrating PIAA coronagraphy in the laboratory to 1e-9 raw contrast at 2 λ/D separation. Recent results from the High Contrast Imaging Testbed (HCIT) at JPL demonstrate contrasts about one order of magnitude from this goal at 2 λ/D. In parallel with our high contrast demonstration at 2 λ/D, we are developing and testing new designs to reduce inner working angle and improve performance in polychromatic light. The newly developed PIAA complex mask coronagraph (PIAACMC) concept provides total starlight extinction and offers full throughput with a sub- λ/D inner working angles. We also describe a recent laboratory demonstration of fine pointing control with PIAA.

Keywords: Exoplanets, Coronagraphy

1. INTRODUCTION

Direct imaging and spectroscopic characterization of habitable exoplanets must overcome the high contrast and small angular separation between the planet and its host star, and must do so while maintaining high photometric efficiency due to the small apparent brightness of the planet. Many coronagraph concepts have recently been proposed to solve this challenge using ground-based or space telescopes[1]. Among the many options proposed, the Phase-Induced Amplitude Apodization (PIAA) coronagraph[2-9] is particularly attractive thanks to the combination of high throughput, high contrast and small inner working angle.

1.1 How Phase-Induced Amplitude Apodization (PIAA) enables high efficiency coronagraphy ?

Many coronagraphs concepts rely on pupil apodization, either as the main technique to suppress diffraction rings in the focal plane image[1], or in combination with a focal plane mask in a configuration similar to a Lyot coronagraph. The conventional technical implementation of pupil apodization relies of selective transmission with a pupil plane mask – a robust but low efficiency solution. The coronagraph design must then trade contrast against efficiency and inner working angle (IWA), a particularly painful choice for exoplanet imaging instruments/missions.

*guyon@naoj.org; phone 1 818 292 8826

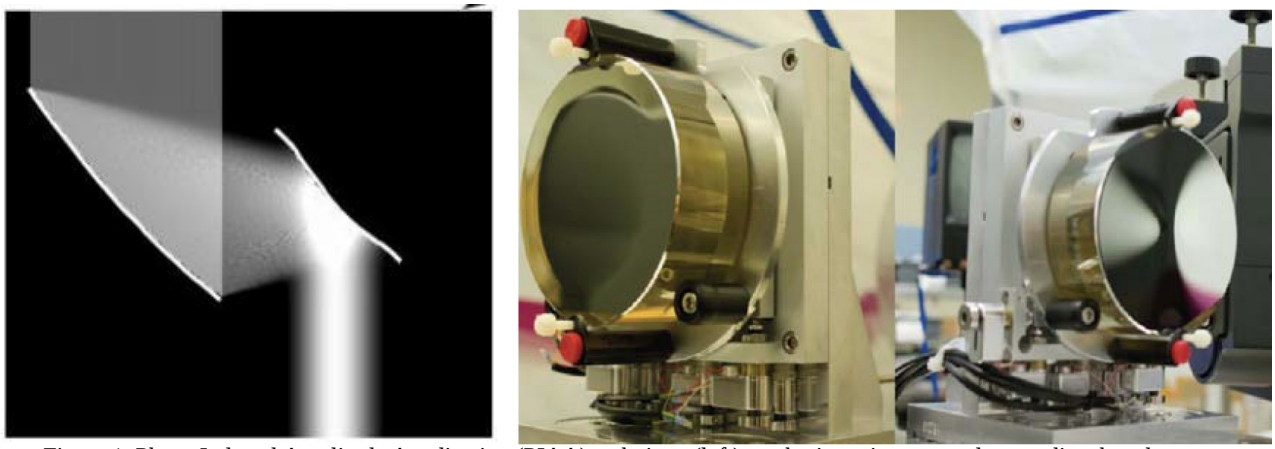

Figure 1. Phase-Induced Amplitude Apodization (PIAA) technique (left): aspheric optics are used to apodize the telescope beam without light loss. Right: Set of PIAA mirrors, Zerodur substrate, manufactured by L3-Tinsley

Phase-Induced Amplitude Apodization (PIAA) achieves the apodization with beam shaping, using aspheric optics such as the ones shown in figure 1, to reshape the telescope beam into an apodized beam with no loss in throughput or angular resolution. This coronagraphic approach offers very high performance, as it combines full throughput, small IWA and full angular resolution. If reflective PIAA optics (aspheric mirrors) are used, chromaticity can be very low. A challenging part of this approach is the manufacturing of the aspheric optics, which sometimes requires a ``hybrid'' approach where apodization is shared between a mild apodizer and PIAA optics. A set of ``inverse'' PIAA optics is also required at the back end of the coronagraph to cancel field aberrations introduced by the first set of PIAA optics. This inverse set plays no role in the coronagraphic process, but considerably extends the field of view over which the PSF is diffraction limited.

2. CURRENT TECHNOLOGY STATUS

2.1 Overview of technology efforts

PIAA coronagraph technologies are being actively developed at NASA Ames Research Center and the Jet Propulsion Laboratory for future use in space missions. These efforts, funded by NASA, are aimed at demonstrating that high contrast can be obtained at or within 2 λ/D with high efficiency, therefore maximizing science return for a fixed telescope diameter. The Jet Propulsion Laboratory (JPL) testbed is operated in vacuum and therefore offers the wavefront stability required to seek the high (~ 1e-9) raw contrast required for direct imaging of exo-Earths. The NASA Ames testbed is operated in a temperature-stabilized air environment, and is complementary to the efforts at JPL, as it enjoys more hardware flexibility. The NASA Ames testbed is better suited for more moderate contrast demonstration with prospective techniques/approaches, and is exploring PIAA-based coronagraphic solutions offering between 1 and 2 λ/D IWA. Such efforts are well suited to the proposed EXCEDE mission[10], for which NASA Ames plays a major role in technology development[11].

2.2 High Contrast Laboratory Results

Figure 2 shows example high contrast images obtained at the NASA Ames and JPL testbeds, and illustrates the complementarity between the testbed activities: the JPL testbed achieves higher contrast thanks to the vacuum environment, while the NASA Ames testbed is exploring solutions for high contrast at smaller IWA. The best contrast value obtained so far at 2 λ/D is 4e-9 at JPL with an somewhat large error bar due to uncertainties in the photometric calibration (the contrast value is between 2e-9 and 8e-9 when taking into account uncertainties). At 1.2 λ/D, the NASA Ames testbed is currently achieving better than 1e-5 contrast. All results are so far in monochromatic light, and limited by stability and wavefront control issues that are independent of the coronagraph concept.

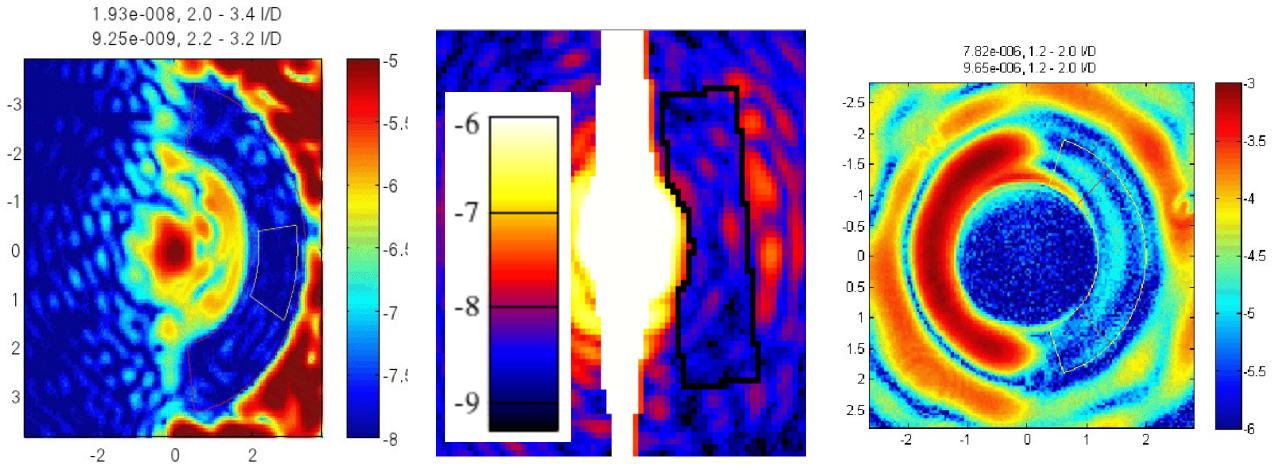

Figure 2. High contrast laboratory PIAA images. Left: NASA Ames testbed image showing contrast at the 1e-8 level from 2 to 3.4 λ/D. Center: High contrast image acquired in vacuum at JPL, reaching 4e-9 average contrast (with a 100% photometric calibration uncertainty: actual contrast value is between 2e-9 and 8e-9) in the zone outlined, extending from 2.0 λ/D (inner radius) to 5.6 λ/D (outer corner). Right: NASA Ames testbed image showing high contrast imaging down to 1.2 λ/D radius.

2.3 Ground-based use of PIAA: the Subaru Coronagraphic Extreme-AO (SCExAO) system

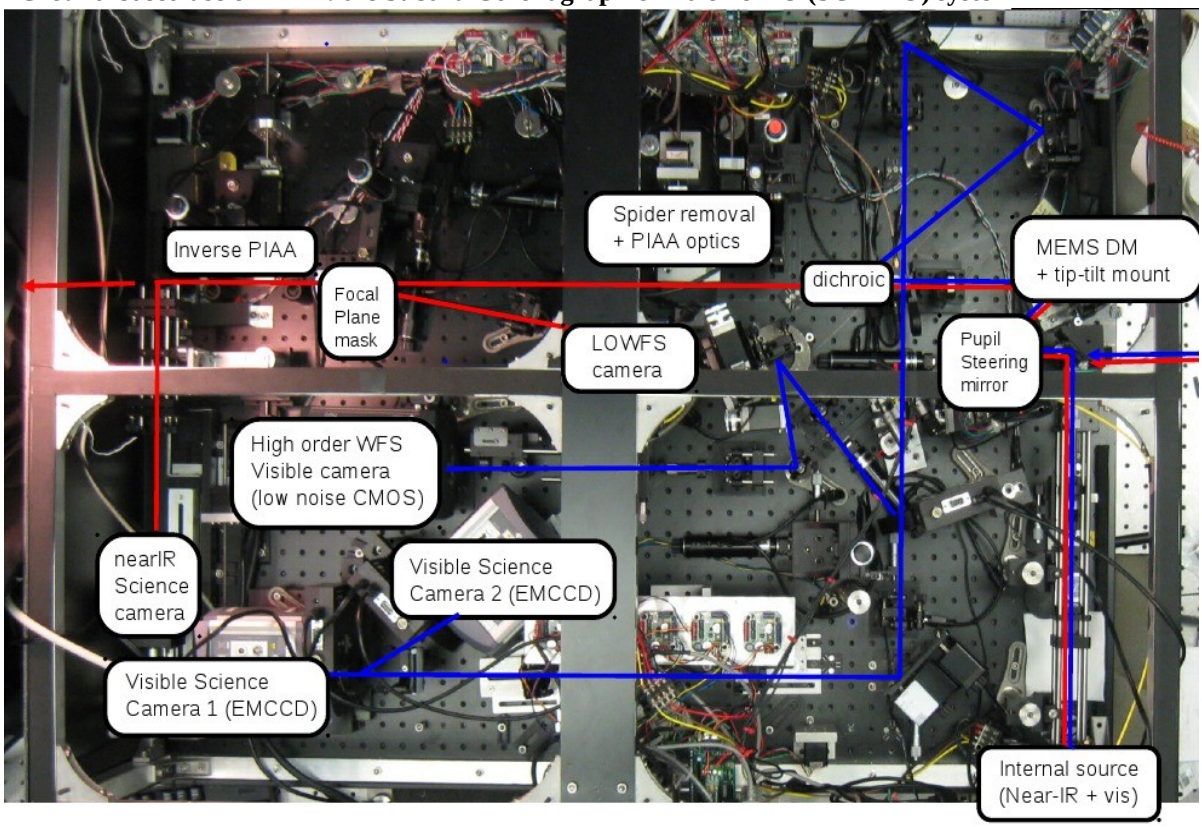

Figure 3. View of the SCExAO instrument bench. Light travels from right to left in this view. The near-IR light path is shown in red; the visible light path is shown in blue. The PIAA coronagraph is located in the center of the near-IR light path.

The PIAA coronagraph is at the core of the Subaru Coronagraphic Extreme-AO (SCExAO) system, under development for the Subaru Telescope. The PIAA's high efficiency and small IWA, combined with Subaru Telescope's 8.2-m aperture, enables high contrast imaging as close as 40mas from the optical axis in the near-IR. The SCExAO instrument, placed downstream of the facility 188-elements curvature adaptive optics system, includes fine wavefront correction and calibration in support of high contrast imaging. SCExAO's PIAA coronagraph architecture includes a coronagraphic low-order wavefront sensor (CLOWFS) and an inverse-PIAA field aberration correction unit. The CLOWFS is described in detail in the next section. Figure 3 shows the SCExAO layout. SCExAO is currently in engineering phase, and has demonstrated on-sky use of the PIAA coronagraph as well as on-sky validation of the CLOWFS. More details on the system can be found in a separate publication[12].

3. POINTING CONTROL WITH PIAA: APPROACH AND LABORATORY DEMONSTRATION

3.1 Pointing requirement

In this section, we establish pointing requirements that should be met using the most aggressive IWA coronagraphs. We conservatively assume that the coronagraph performance is limited by stellar angular size, not by the coronagraph design or performance. This assumption leads to the most demanding requirements, and requirements could be relaxed for coronagraph designs (including some flavors of PIAA) that are not reaching the stellar angular size limit.

For the lowest IWA coronagraphs, the **pointing jitter requirement** at the coronagraph focal plane mask is ultimately set by the angular size of the target star: reducing pointing jitter well below the stellar angular radius does not improve contrast. On a 2 m diameter telescope, a 0.01 λ/D RMS pointing jitter corresponds to 0.5 milli-arcsecond (mas) at optical wavelengths, which is the radius of a Sun-like star at 10 pc distance. Achieving a RMS pointing jitter below this level therefore ensures that the coronagraph leak due to pointing errors is no more than the light leak due to the finite stellar angular size for telescope diameters of 2 m or more.

The second pointing requirement in coronagraphs is a **pointing calibration requirement**. While the first goal (RMS jitter) ensures that the contribution of pointing errors is not a significant source of photon noise, this second goal ensures that pointing errors cannot produce planet detection false positives. Residual tip-tilt errors in the coronagraph should be calibrated to 0.003 λ/D in order to allow calibration of coronagraphic leaks due to pointing errors to a 10e−11 contrast level on a small IWA coronagraph designed to operate the the limit imposed by stellar angular size.

3.2 The Coronagraph Low-Order Wavefront Sensor (CLOWFS): Principle

The approach for accomplishing the goals listed in section 3.1 is to implement and operate a dedicated sensor, the Coronagraphic Low-Order Wave-Front Sensor[13] (CLOWFS), which uses starlight otherwise rejected by the coronagraph. Using the light that falls on the central (within the coronagraph IWA) part of the focal plane mask offers two fundamental advantages over schemes relying on analysis of coronagraphic science images for pointing control:

- A large number of photons is available for the measurement, allowing fast and accurate tip-tilt estimation
- Pointing errors can be measured before they start producing coronagraphic leaks in the science image

3.3 Implementation and Laboratory Results

The pointing demonstration was performed on the existing PIAA coronagraph table which is currently in the vacuum Micro-Arcsecond Metrology (MAM) chamber at JPL. The CLOWFS implementation for this milestone closely follows the design described in the original CLOWFS publication[13]. The only significant difference is that only one defocused image is acquired by the CLOWFS camera, while the original CLOWFS assumes two images are acquired. This simplification has no impact on the CLOWFS tip-tilt functionality or performance.

Figure 4 shows the result of the pointing demonstration. For this test, pointing disturbances were intentionally added to the testbed, and measured by the CLOWFS. The test consists of two measurement sequences: a measurement sequence in open loop (no correction), followed by a measurement in closed loop (with correction). The input disturbance sent to the testbed was the same for both measurements. The RMS pointing error was reduced by a factor 81, from 87e-3 λ/D to

1.07e-3 λ/D. The value obtained after correction is about 10 times lower than the typical stellar angular size for a medium-sized (≈ 2-m) telescope in visible light, therefore validating that pointing can be measured and controlled sufficiently well to become a minor term in the contrast error budget.

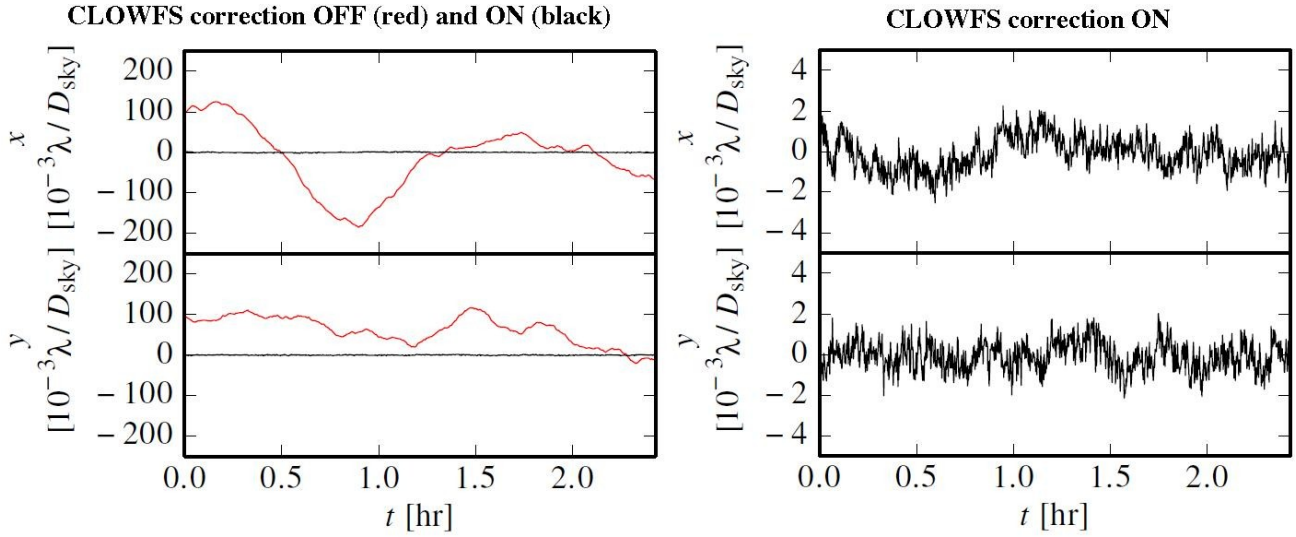

Figure 4. Results obtained in the laboratory with the CLOWFS. The CLOWFS pointing measurement as a function of time is shown on the left with the correction off (red curve) and on (black curve around zero value). At the vertical scale used on the left, the corrected pointing value curves are nearly indistinguishable from a zero valued straight line. On the right, the corrected pointing value curves are shown with a vertical scale 50 times finer than on the left. The quadrature sums of x and y RMS residuals are 87e-3 and 1.07e-3 λ/D for the correction OFF and correction ON cases respectively.

Separately from the pointing RMS value test described above, open loop tests were conducted to measure the CLOWFS response to small signals and the cross-talk between the X and Y axes. These tests showed that the CLOWFS can reliably measure pointing offsets at the 1e-4 λ/D level, provided that measurement noise (photon noise and readout noise) are sufficiently small.

4. PIAACMC: APPROACHING THE FUNDAMENTAL PERFORMANCE LIMIT OF CORONAGRAPHY

4.1 PIAACMC Principle

The simplest form of PIAA coronagraph, which we call the PIAAC, is one where the lossless apodization is used to produce a PSF with minimal diffraction wings. The central bright part of this PSF is then blocked by an opaque focal plane mask to remove starlight while preserving light from nearby sources. An inverse PIAA set may then be used to recover a sharp diffraction-limited image over a useful field of view. This scheme is shown at the top of figure 5.

The same lossless PIAA technique can also be used to replace the apodizer in coronagraph architectures where the starlight rejection is shared between several components (instead of relying entirely on the opaque focal plane mask). This leads to PIAA coronagraph types with higher performance, as the flexibility of using several masks for starlight rejection opens new possibilities. For example, an apodized pupil Lyot coronagraph (APLC) configuration with a PIAA front end is especially attractive, as the full throughput apodization of the PIAA optics greatly enhances the APLC's performance. This coronagraph architecture is shown in the center of figure 5. Performance can be further improved by allowing the focal plane mask to be smaller, partially transmissive and phase-shifting. This allows total on-axis coronagraphic extinction, and a very small IWA. This approach, shown in the bottom of figure 5, is referred to as the PIAA Complex Mask Coronagraph (PIAACMC). The PIAACMC concept[14] is, theoretically, the highest performance

coronagraph, as it can fully suppress starlight (contrast entirely limited by wavefront control and manufacturing limits) with an inner working angle equal to 0.64 λ/D.

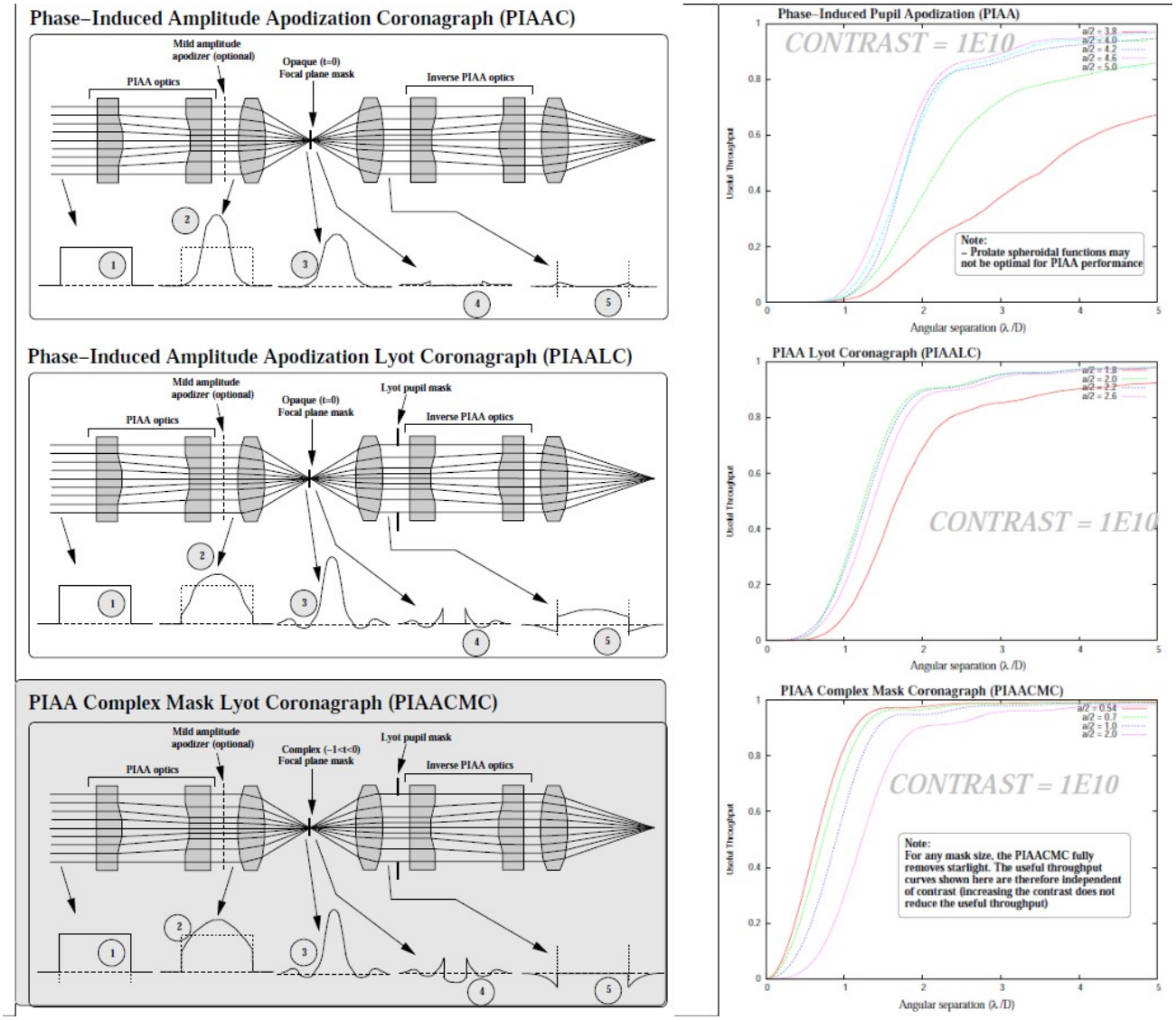

Figure 5. PIAA-based coronagraph architectures (left) and corresponding theoretical performance (right). The coronagraph performance is shown as a useful throughput vs. angular separation curve for a 1e10 contrast. The highest performance architecture is the PIAACMC, currently under active development.

4.2 Challenges, performance limitations

As a high performance coronagraph with small IWA (less than 1 λ/D), the PIAACMC is extremely sensitive to low order aberrations, and pointing needs to be extremely well controlled at the focal plane mask. As demonstrated in section 3, this challenging requirement can be met with the CLOWFS, which offers sufficiently good pointing control to reach the fundamental performance limit imposed by the stellar angular radius.

Stellar angular size does indeed put strong limits on the performance achievable with the PIAACMC. With a telescope 4 m or larger, in visible light, the stellar angular size of nearby stars is too large to allow 1e10 contrast with a 1 λ/D IWA. The PIAACMC's benefit is then to (1) allow imaging of inner planets around nearby stars, but the raw contrast level

requires long exposure times to overcome photon noise, and (2) increase sample size by allowing detection of planets around more distant stars requiring small IWA. The PIAACMC is most valuable for small telescopes, as it can then offer sub λ/D IWA with nearly full throughput.

Managing chromatic effects is essential in the PIAACMC: the focal plane mask is required to introduce both a phase offset and a partial transmission – both of which need to be well controlled as a function of wavelength. The mask size is also critical, as, unlike the conventional PIAA coronagraph, its role is not simply to block starlight: the right amount of starlight needs to fall within the mask so that it can destructively interfere with light outside the focal plane mask. Our approach to solving this challenge is to design a focal plane mask which maintains constant complex amplitude (phase, amplitude) across the desired spectral range but changes size linearly with wavelength. The mask can be designed as a zeroth order diffraction grating consisting of multiple cells, each smaller than λ/D.

5. PIAACMC FOR SEGMENTED AND CENTRALLY OBSCURED PUPILS

We show in this section that the PIAACMC concept described in section 4 can be applied to segmented and centrally obscured pupils with no loss in performance. The fact that a high performance coronagraph concept, approaching the fundamental performance limit of coronagraphy, is compatible with any pupil geometry has significant implications for planning future high contrast imaging missions. Future large segmented telescopes, or existing centrally obscured telescopes, could be used to their full potential. We describe in this chapter how PIAACMC can be designed for non-circular pupils, and show a few example designs.

5.1 Principle

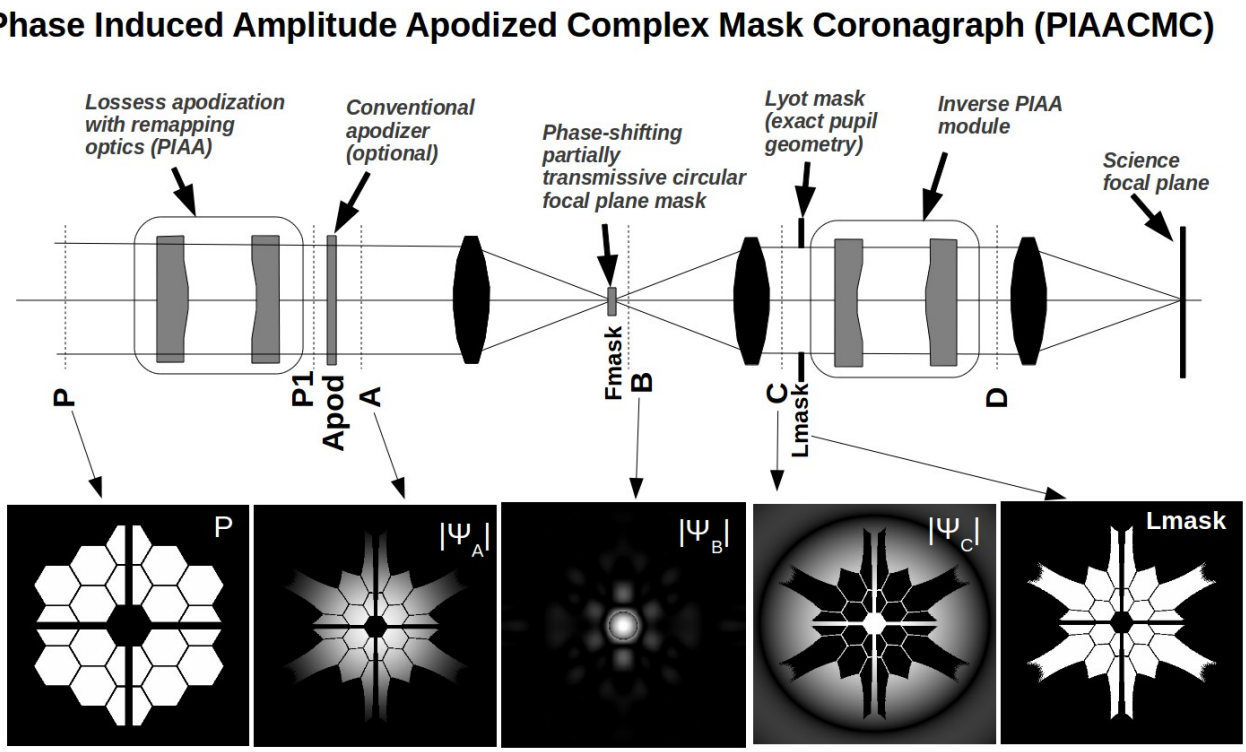

Figure 6. PIAACMC principle applied to a segmented aperture. See text for details.

An example PIAACMC design is shown in figure 6 for a segmented centrally obscured pupil. The entrance pupil P (image shown in the lower left of the figure) is apodized with lossless aspheric PIAA optics. Because the PIAA optics perform apodization by remapping instead of selective transmission, the resulting pupil P1 shape is modified. A

conventional apodizing mask may be used to fine-tune the apodization if the PIAA optics do not exactly produce the required amplitude distribution (this will be addressed in the following section). The resulting pupil A is shown in the second image from the lower left corner. The image of an on-axis point source is shown in the center image, where the phase-shifting partially transmissive focal plane mask is inserted. In the output pupil plane C, all light within the pupil has been removed, while diffracted starlight fills the gap and obstructions of the segmented pupil. A Lyot mask (noted Lmask) can then select only the geometric pupil area (after remapping) to fully block on-axis starlight while fully transmitting the light from distant off-axis source. A well-documented side-effect of apodization with PIAA optics is that off-axis PSFs are highly distorted, and corrective optics (inverse PIAA) are required at the output of the coronagraph to maintain diffraction limited sharp PSFs over a scientifically useful field of view[15].

5.2 PIAACMC design process

A PIAACMC is designed by performing a lossless PIAA apodization of the pupil to produce a generalized prolate function for the aperture. In the unobstructed circular pupil case, designing the PIAACMC is relatively simple, as PIAA apodization using a radial remapping function preserves the circular aperture shape[14]. The prolate function can thus be first computed, and then realized with a radial PIAA apodization.

Designing a PIAACMC for complex shaped apertures is considerably more challenging because the PIAA apodization modifies the aperture shape, which itself changes the generalized prolate function. In addition to this circular problem, if the aperture is not circularly symmetric, the generalized prolate is also not symmetric, and the required remapping function therefore cannot be written as a radial function. While PIAA optics can be designed for any radial remapping, an arbitrarily chosen 2D remapping function can almost never be realized with a set of two PIAA optics.

To overcome the two challenges listed above (circular design problem due to effect of PIAA on aperture shape, and complexity/impossibility of designing PIAA optics for non-circular symmetric remapping), a hybrid PIAACMC design is adopted, which includes a conventional apodizer after the remapping to produce the required prolate function. Thanks to this post-apodizer, the output of the PIAA apodization does not need to exactly match the generalized prolate function, allowing radial remapping functions to be used on non-circular symmetric apertures. The goal of the design optimization is to bring the PIAA apodization and generalized prolate functions close, in order to minimize the strength of the post-apodizer and thus maintain a high system throughput.

The proposed steps for designing a PIAACMC for complex shaped apertures are :

1. Choose radial remapping function $r1=f_b(r0)$. For convenience, the remapping function is selected among a pre-computed set of functions used to produce prolate spheroidal apodizations on circular apertures. The focal plane mask diameter corresponding to the prolate spheroidal function is denoted *b*, and the corresponding remapping function and apodization intensity profile are respectively f_b and I_b.
2. Apply the remapping function to the complex shaped entrance pupil. The remapping transforms the entrance pupil intensity $P(x,y)$ into $P_1(x,y)$.
3. Choose a focal plane mask diameter *a*.
4. Compute the generalized prolate function $Prol_a(x,y)$ for the remapped aperture shape defined by $P_1(x,y)>0$, using the focal plane mask diameter *a*. This is done iteratively by Fourier transforms and clippings.
5. Compute the amplitude ratio $Apo(x,y)=Prol_a(x,y)/P_1(x,y)$. This is the post-apodizer amplitude transmission function. $Apo(x,y)$ is then scaled to ensure that its maximum value is equal to 1. The intensity-weighted average of $Apo(x,y)^2$ defines the coronagraph throughput for off-axis sources.

Steps (3) to (5) are repeated for different values of the focal plane mask size *a*. The off-axis coronagraph throughput is computed for each choice of *a*, and the final focal plane mask size is chosen to maximize throughput. This optimization links the choice of the remapping function (step (1)) to a value of the focal plane mask radius *a*. For a circular unobstructed aperture, the solution would be *a*=*b*, for which the PIAA apodization would perfectly match the generalized prolate function. On arbitrarily shaped pupils, the focal plane mask radius is usually close to, but not equal to, *b*. Stronger apodization functions correspond to larger values for *a* and *b*.

5.3 Example designs for ground-based telescope pupils

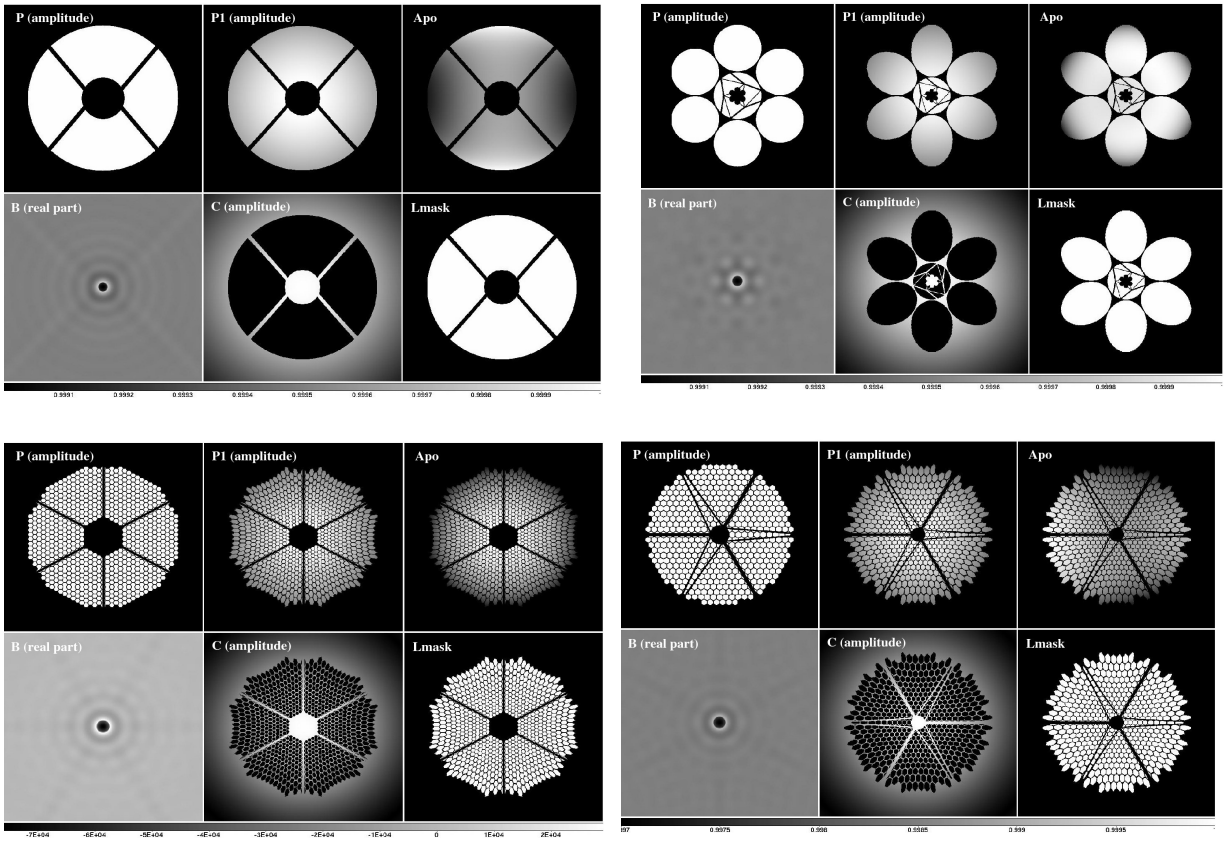

Figure 7. PIAACMC designs for centrally obscured and segmented apertures. Top left: Subaru pupil. Top rigt: The Giant Magellan Telescope pupil, representative of an aperture with few segments. Bottom left: The European-ELT pupil. Bottom right: The Thirty Meter Telescope (TMT) pupil, representative of a highly segmented pupil. Within each of the four panels, the input pupil (top left), the remapped pupil P1 (top center), the conventional apodization mask (top right) the real part of the focal plane complex amplitude including the focal plane mask (bottom left), the output pupil amplitude (bottom center) and the Lyot mask geometry (bottom right) are shown.

Figure 7 shows example PIAACMC designs for centrally obscured and segmented pupils. In each case, the coronagraph achieves total extinction of an on-axis point source and sub-λ/D IWA. Table 1 gives a list of coronagraph designs for the same pupil geometries. The table entries corresponding to figure 7 are: Subaru #1, GMT #1, TMT #1 and E-ELT #1. The last two columns of table 1 show the main performance metrics for the coronagraphs: throughput and IWA.

Table 1. Example PIAACMC designs for centrally obscured and segmented pupils.

Design	PIAA function (b/2)	PIAA strength (Imax/Imin)	Focal plane mask radius (a/2)	Focal plane mask transmission	Throughput	IWA
Subaru #1	0.6 λ/D	2.42	0.603 λ/D	84.24%	99.91%	0.67 λ/D
Subaru #2	1.2 λ/D	26.83	1.33 λ/D	2.06%	97.04%	1.11 λ/D
GMT #1	0.7 λ/D	3.3	0.693 λ/D	98.55%	99.98%	0.72 λ/D
GMT #2	1.2 λ/D	26.83	1.12 λ/D	20.71%	99.47%	0.89 λ/D
GMT #3	1.5 λ/D	124.09	1.32 λ/D	16.64%	99.14%	0.92 λ/D
TMT #1	0.8 λ/D	4.69	0.797 λ/D	85.51%	99.80%	0.78 λ/D
TMT #2	1.2 λ/D	26.83	1.16 λ/D	32.46%	99.80%	0.94 λ/D
TMT #3	1.5 λ/D	124.09	1.394 λ/D	27.73%	99.80%	0.99 λ/D
E-ELT #1	0.8 λ/D	4.69	0.816 λ/D	99.87%	97.77%	0.81 λ/D
E-ELT #2	1.2 λ/D	26.83	1.15 λ/D	45.58%	99.50%	0.93 λ/D
E-ELT #3	1.5 λ/D	124.09	1.37 λ/D	37.85%	99.42%	0.98 λ/D

6. CONCLUSIONS

Recent laboratory results have demonstrated that coronagraphs based on the PIAA technique can reach high contrast at small IWA, while preserving the full sensitivity and angular resolution of the telescope. A significant recent achievement has been the laboratory demonstration that instrument pointing can be controlled to better than 1e-3 λ/D – a level of pointing that is usually not required. This result, obtained with a coronagraphic low-order wavefront sensor (CLOWFS) is directly applicable to several other coronagraph concepts.

In parallel to laboratory demonstrations, recent improvements in the PIAA-based coronagraph concepts show that sub-λ/D IWA coronagraphy is possible, provided that the stellar angular size is sufficiently small to allow it, and that chromatic effects can be mitigated (development of a solution to this last challenge is ongoing). The high efficiency PIAACMC concept was also recently shown to be compatible with segmented and centrally obscured pupils, with no loss of performance.

ACKNOWLEDGMENTS

This work was funded by NASA Technology Demonstration for Exoplanet Missions (TDEM) program., the National Astronomical Observatory of Japan (NAOJ), and the Japanese Society for the Promotion of Science (JSPS).

REFERENCES

[1] Guyon, O., Pluzhnik, E. A., Kuchner, M. J., Collins, B., and Ridgway, S. T., “Theoretical Limits on Extrasolar Terrestrial Planet Detection with Coronagraphs,” ApJS 167, 81–99 (2006).

[2] Guyon, O., “Phase-induced amplitude apodization of telescope pupils for extrasolar terrestrial planet imaging,” A&A 404, 379–387 (2003).

[3] Traub, W. A. and Vanderbei, R. J., “Two-Mirror Apodization for High-Contrast Imaging,” ApJ 599, 695-701 (2003).
[4] Guyon, O., Pluzhnik, E. A., Galicher, R., Martinache, F., Ridgway, S. T., and Woodruff, R. A., “Exoplanet Imaging with a Phase-induced Amplitude Apodization Coronagraph. I. Principle,” ApJ 622, 744–758 (2005).
[5] Vanderbei, R. J. and Traub, W. A., “Pupil Mapping in Two Dimensions for High-Contrast Imaging,” ApJ 626, 1079–1090 (2005).
[6] Vanderbei, R. J., “Diffraction Analysis of Two-dimensional Pupil Mapping for High-Contrast Imaging,” ApJ 636, 528–543 (2006).
[7] Martinache, F., Guyon, O., Pluzhnik, E. A., Galicher, R., and Ridgway, S. T., “Exoplanet Imaging with a Phase-induced Amplitude Apodization Coronograph. II. Performance,” ApJ 639, 1129–1137 (2006).
[8] Pluzhnik, E. A., Guyon, O., Ridgway, S. T., Martinache, F., Woodruff, R. A., Blain, C., and Galicher, R., “Exoplanet Imaging with a Phase-induced Amplitude Apodization Coronagraph. III. Diffraction Effects and Coronagraph Design,” ApJ 644, 1246–1257 (2006).
[9] Belikov, R., Kasdin, N. J., and Vanderbei, R. J., “Diffraction-based Sensitivity Analysis of Apodized Pupil-mapping Systems,” ApJ 652, 833–844 (2006).
[10] Guyon, O., Schneider, G. H., Belikov, R., and Tenerelli, D. J., “The EXoplanetary Circumstellar Environment and Disk Explorer (EXCEDE)”, Society of Photo-Optical Instrumentation Engineers (SPIE) Conference Series 8842 (2012).
[11] Belikov, R., Pluzhnik, E., Witteborn, F. C., Greene, T. P., Lynch, D. H., Zell, P. T., Schneider, G. H., Guyon, O., “EXCEDE technology development I: first demonstrations of high contrast at 1.2 λ/D for an Explorer Space Telescope Mission”, Society of Photo-Optical Instrumentation Engineers (SPIE) Conference Series 8842 (2012).
[12] Martinache, F., Guyon, O., Clergeon, C. S., Garrel, V., “The Subaru coronagraphic extreme-AO project: first observations” Society of Photo-Optical Instrumentation Engineers (SPIE) Conference Series 8847 (2012).
[13] Guyon, O., Matsuo, T., and Angel, R., “Coronagraphic Low-Order Wave-Front Sensor: Principle and Application to a Phase-Induced Amplitude Coronagraph,” ApJ 693, 75–84 (2009).
[14] Guyon, O., Martinache, F., Belikov, R., and Soummer, R., “High Performance PIAA Coronagraphy with Complex Amplitude Focal Plane Masks,” ApJS 190, 220–232 (2010).
[15] Lozi, J., Martinache, F., Guyon, O., “Phase-Induced Amplitude Apodization on Centrally Obscured Pupils: Design and First Laboratory Demonstration for the Subaru Telescope Pupil”, PASP, Vol 121, pp. 1232-1244 (2009).